THE ASTROPHYSICAL JOURNAL, 509:366–378, 1998 December 10

ABUNDANCE ANALYSES OF FIELD RV TAURI STARS. IV. AD AQUILAE, DS AQUARII, V360 CYGNI, AC HERCULIS, AND V453 OPHIUCHI

SUNETRA GIRIDHAR
Indian Institute of Astrophysics, Bangalore, 560034 India; giridhar@iiap.ernet.in
DAVID L. LAMBERT
Department of Astronomy, University of Texas, Austin, TX 78712; dll@astro.as.utexas.edu
AND
GUILLERMO GONZALEZ
Department of Astronomy, University of Washington, Seattle, WA 98195; gonzalez@astro.washington.edu
Received 1998 April 7; accepted 1998 July 16

ABSTRACT

Abundance analyses are presented and discussed for five RV Tauri variables. Three stars—DS Aqr, V360 Cyg, and V453 Oph—are RV C stars by spectroscopic classification, i.e., metal lines are weak. They are shown to be metal poor with [Fe/H] from −1.0 to −2.2 with normal relative abundances of other elements. By contrast, AD Aql and AC Her are RV B stars with an odd abundance pattern: elements that condense into grains at a high temperatures are underabundant (i.e., [Fe/H] = −2.1 for AD Aql) but elements with a low condensation temperatures are much less underabundant (i.e., [S/H] = 0.0 and [Zn/H] = −0.1 for AD Aql). This abundance pattern is ascribed to a separation of dust and gas in the upper atmosphere of the star. The present analyses with previously published results are used to investigate the systematics of the dust-gas separation in RV Tauri variables. The process is apparently inoperative in stars with an initial metallicity of about [Fe/H] $\lesssim -1.0$; RV C stars and similar variables in globular clusters are immune to the dust-gas separation. The process achieves more severe effects in RV B than in RV A stars. The strength of the abundance anomalies attributed to dust-gas separation is not correlated with reported infrared excesses. After correction for the effects of the dust-gas separation, there is no strong evidence from the abundances that evolution along the AGB and experience of the third dredge-up preceded the formation of the majority of the RV Tauri variables.

Subject headings: circumstellar matter — stars: abundances — stars: variables: other (RV Tauri)

1. INTRODUCTION

In this series of papers, we have been exploring the chemical compositions of RV Tauri variables in the Galactic field. At the outset, we supposed that data on the compositions of the RV Tauri variables could be used to explore the changes of composition made as the star evolved from the main sequence to its present advanced age. The atmospheric pulsations were naively supposed to be no more than a nuisance with a possible offsetting opportunity. Presence of a shock in the atmosphere leads to a doubling of absorption line profiles at particular phases. This doubling is to us a nuisance in that such spectra must be discarded because available models do not pretend to represent disturbed atmospheres. At other phases, standard abundance analyses seem possible and offer the opportunity to demonstrate that analyses at quite different phases return very similar abundances.

It is often supposed that RV Tauri variables evolve off the asymptotic giant branch (AGB) and evolve into post-AGB stars such as protoplanetary nebulae before descending the white dwarf cooling track. Then, the composition of a RV Tauri variable should betray happenings in its AGB predecessor. Our first paper (Giridhar, Rao, & Lambert 1994), an analysis of IW Car, shattered this expectation. The atmosphere did not have a normal composition but was highly depleted in those elements that condense at "high" temperatures (∼1500 K) into dust grains. Our interpretation was that a separation of dust from gas was occurring in the stellar wind driven from the dusty circumstellar shell that is known to be responsible for the large infrared excess of this star. Circulation of gas between the photosphere and the inner regions of the circumstellar shell led to a gradual depletion in the photosphere of those elements that make up the grains. This circulation is presumably controlled by atmospheric pulsations: gas is propelled above the photosphere at one phase in the pulsation, and gas depleted of elements that condensed into grains falls back to the photosphere at a later phase. Discovery of an anomalous composition led to spectroscopic pursuit of other field RV Tauri variables. Depletion of metals by dust-gas separation was found to be a common property (Gonzalez, Lambert, & Giridhar 1997a, 1997b). Variables in metal-poor globular clusters, however, were shown to have the same metal abundances as the red giants of these clusters (Gonzalez & Lambert 1997; Russell 1997), i.e., dust-gas separation had not operated in the cluster variables. For those stars in which the dust-gas separation is active, the signature left by deep mixing in the AGB star is modified or even erased by the dust-gas separation. Abundances and pulsations are now seen to comprise a unified grand puzzle.

To explore this puzzle we decided to analyze a more diverse sample of RV Tau variables. In the spectroscopic classification introduced by Preston et al. (1963), RV A stars are the cooler RV Tau variables having spectral types of G–K; RV B stars are the warmer stars that Preston et al. refer to as "Fp(R)" variables, where the letter "R" indicates, as is customary in spectral classification, the presence in low-dispersion spectra of enhanced bands of CN and CH; RV C stars are distinguished by their weak or absent bands of CH and CN. Our earlier papers did not include

TABLE 1

THE PROGRAM STARS

Quantity	AD Aql	DS Aqr	V360 Cyg	AC Her	V453 Oph
V (mag)[a]	11.3–12.1	10.3–11.6	11.1–13.4	7.3–8.3	10.3–11.3
$B-V$ (mag)[a]	0.75	0.54	0.84	0.79	0.90
$E(B-V)$ (mag)[b]	...	0.00	0.26	0.14	0.45
Spectral Type[c]	G8	F2	F8	F8	Fp
Period (days)[c]	65.4	78.3	70.5	75.5	91.0
Spectroscopic group[d]	RV B?	RV C	RV C	RV B	RV C
Photometric type[c]	RV a	RV a	RV a	RV a	RV a

[a] Data from Wahlgren 1992 and Pollard et al. 1996.
[b] Data from Goldsmith et al. 1987 and Pollard et al. 1996.
[c] Data from the GCVS.
[d] Data from Preston et al. 1963 and Lloyd Evans 1985.

field RV C stars. Since a high radial velocity is common among these stars (Joy 1952), it is likely that the majority are of intrinsically low metallicity and, therefore, might like the globular cluster variables not be subject to the effects of a dust-gas separation. To test this conjecture, we include here analyses of three field RV C stars (DS Aqr, V360 Cyg, V453 Oph).[1]

Photometrically, the RV Tau stars have periods in the range 50–150 days with a pattern of alternating deep and shallow minima. A photometric subclassification is available: two subgroups—RV a and RV b (Kukarkin et al. 1958)—are recognized. The mean magnitude of the RV a stars appears constant but that of the RV b stars varies on a long timescale ($\sim$600–2600 days). This slow modulation has been ascribed to the presence of the variable in a binary system. A model involving eclipse of the RV Tau star by dust that it recently or not so recently ejected has been drawn by Percy (1993), Waelkens & Waters (1993), and Fokin (1994). This picture is criticized adversely by Pollard et al. (1996) as incompatible with the color variations. Pollard et al. invoke an interacting binary with an orbital phase-dependent interaction occurring between the RV Tau star and either its companion or material previously ejected. The interaction is suggested to control the mass ejection by the RV Tau star.

Detection of spectroscopic binaries is exceedingly difficult for RV Tauri variables as a small orbital variation of velocity must be extracted in the presence of a larger pulsational variation that is rarely adequately sampled. Post-AGB stars exhibiting severe effects of dust-gas separation are now known to be spectroscopic binaries (Van Winckel, Waelkens, & Waters 1995). This correspondence leads to speculations that dust-gas separation might be enhanced in RV b stars relative to RV a stars, and that the metal depletion of post-AGB stars, now beyond the blue edge of the instability strip, might have originated a few hundred to a few thousand years earlier, when the stars were RV Tau variables.

2. OBSERVATIONS

High-resolution spectra of the stars listed in Table 1 were acquired with two telescopes at the W. J. McDonald Observatory. Spectra of DS Aqr, V360 Cyg, AC Her, and V453 Oph were obtained at the 2.1 m Struve reflector with the CCD-equipped Sandiford Cassegrain echelle spectrograph (McCarthy et al. 1993). A typical spectrum has a signal-to-noise ratio (S/N) in the continuum of 80–100 and a spectral resolving power of about 50,000. These observations were made between 1994 and 1996. Spectral coverage is described below in the discussions of the individual stars. AD Aql and AC Her were observed at the 2.7 m Harlan J. Smith reflector with the CCD-equipped "2dcoudé" spectrograph (Tull et al. 1995). A spectral resolving power of 60,000 was used and a broad spectral range was covered in a single exposure. Spectra were reduced with the standard packages in NOAO IRAF.

A selection of available spectra was analyzed. Spectra were rejected if they showed line doubling, markedly asymmetric lines, or strong emission at Hβ. It is presumed that the spectra not showing these characteristics represent the atmosphere at its most stable time when standard theoretical models may be applicable.

3. ABUNDANCE ANALYSES

Spectra were analyzed as described by Gonzalez et al. (1997a, 1997b). Equivalent widths of selected unblended weak to moderate strength lines were converted to abundances using an upgraded version of the local thermodynamic equilibrium (LTE) line analysis program MOOG (Sneden 1973). Model atmospheres were taken from a grid computed using the program MARCS (Gustafsson et al. 1975); the Kurucz model atmospheres were used by Gonzalez et al. A normal helium abundance, He/H = 0.1 by number of atoms, is assumed. Atmospheric parameters—effective temperature $T_{\rm eff}$, surface gravity log g, metallicity [Fe/H], and microturbulence ξ_t—were derived in the customary manner from the suite of measured Fe I and Fe II lines. The gf-values of the Fe I lines were taken from Lambert et al. (1996) or estimated using the precepts listed in that paper. For Fe II, the gf-values were taken from the Giridhar & Arellano Ferro (1995) compilation. The gf-values of other elements were taken from a compilation by R. E. Luck (1994, private communication). Table 2 lists the atmospheric parameters obtained for all stars from the useful spectra.

Spectral coverage was extensive for AD Aql and AC Her allowing us to measure large numbers of lines including weak lines with central depths of just 2%–4% of the continuum. For these two stars, $T_{\rm eff}$ and log g could be estimated with accuracies of $\pm$150 K and 0.15 dex, respectively. The microturbulence is accurate to 0.2 km s^{-1}. For the other stars, the wavelength coverage was less extensive and the line selection more restricted. In these cases, $T_{\rm eff}$ is estimated accurate to $\pm$200 K and log g to $\pm$0.25 dex with a slight reduction in the accuracy of ξ_t to $\pm$0.3 km s^{-1}. Iron abun-

[1] Some authors associate the classes RV A and B with different metallicities. On the basis of meager data, Preston et al. thought that the RV B stars belonged to a disk-type population with the RV A stars. It was not suggested that RV B stars are metal poor relative to the RV A stars.

TABLE 2

STELLAR PARAMETERS DERIVED FROM THE Fe-LINE ANALYSES

STAR	UT DATE	PULSATION PHASE	MODEL PARAMETER[a]				Fe I[b]		Fe II		COMMENTS
			$T_{\rm eff}$	log g	[Fe/H]	ζ_t (km s^{-1})	log ϵ	n	log ϵ	n	
V360 Cyg	1994 Jun 25	0.68	5250	1.00	−1.4	5.5	6.02 ± 0.15	27	6.08 ± 0.08	9	Weak emission in Hβ
	1994 Sep 13	0.34	5300	1.75	−1.3	3.8	6.15 ± 0.10	27	6.21 ± 0.09	7	Two strong emission, comp. in Hα
DS Aqr.....	1995 Dec 11	0.80	6500	2.00	−1.0	4.0	6.49 ± 0.13	19	6.50 ± 0.10	9	Weak emission in Hα
V453 Oph.....	1994 Aug 16, 18	0.40	5800	0.75	−2.1	3.5	5.34 ± 0.12	40	5.37 ± 0.08	9	Two strong emission, comp. in Hα
AD Aql	1997 Jul 25	0.87	6300	1.25	−2.1	3.5	5.39 ± 0.10	24	5.37 ± 0.09	21	Hα has P-Cygni profile, no emission in Hβ
AC Her	1996 Apr 9, 10, 11	0.70	6000	1.25	−1.4	4.0	6.06 ± 0.11	51	6.05 ± 0.12	9	Hα shows two emission comp., asymmetry in Hβ
	1997 Jun 20	0.47	5800	1.00	−1.3	4.2	6.11 ± 0.12	64	6.13 ± 0.10	22	Hα shows P-Cygni, structure, asymmetry, in Hβ

[a] $T_{\rm eff}$ in K, log g in cgs, [Fe/H] in dex.

[b] log ϵ is the mean abundance relative to H (with log $N_{\rm H} = 12.00$). The solar value of log ϵ (Fe) is 7.50. The standard deviations of the means, as calculated from the line-to-line scatter, are given. n is the number of considered lines.

dances are estimated to be accurate to ± 0.12 to 0.15 dex for AD Aql and AC Her and to ± 0.15 to 0.20 dex for the other three stars. Effects on the other abundances of changing atmospheric parameters by these amounts may be gauged from Table 4 of Gonzalez et al. (1997a). Except for elements represented by one or two weak lines, the error of the mean abundance as estimated from the line-to-line scatter of the abundances is less than the systematic errors from the uncertain atmospheric parameters. Therefore, we do not give the errors of the mean abundances in Table 4; they may be computed from tables that give the line lists. In the case of the metal-depleted stars, the pattern of elemental abundances does not resemble that assumed in the construction of the MARCS atmospheres, but we have checked that this difference has little effect on the derived abundances.

4. CHEMICAL COMPOSITIONS

Three signatures may be looked for in the chemical compositions: (1) the initial composition, (2) the effects of deep mixing during stellar evolution on the initial composition, and (3) the effects of the dust-gas separation. The signature of the initial composition may be anticipated from published studies on less evolved stars that show a generally smooth run of $[X/\mathrm{Fe}]$ with [Fe/H], at least over the metallicity range considered appropriate for field RV Tauri variables—see reviews by Lambert (1989), Wheeler, Sneden, & Truran (1989), and McWilliam (1997).[2] Deep mixing affects the light elements (primarily C, N, and O with, perhaps, a modest effect on Na) and the heavy or *s*-process elements. As our earlier papers showed, the dust-gas separation severely depletes those elements having a high condensation temperature (e.g., Ca, Ti, and Fe) but not those of low condensation temperature (e.g., S and Zn, as well as C, N, and O). In the following sections, we discuss how these three effects appear to have conspired to set the sometimes unusual composition of a RV Tauri variable.

4.1. *The RV B Star AD Aquilae*

AD Aquilae is a RV B star of photometric type RVa. Pollard et al. (1996) provide a recent photometric study with limited spectroscopic observations (Pollard et al. 1997). Our analysis uses a spectrum obtained on 1997 July 25 with the 2dcoudé spectrograph. The Pollard et al. (1996) ephemeris gives the phase as 0.87.[3] Hα has a P Cygni profile, as it does throughout its cycle according to a set of profiles published by Pollard et al. (1997). The velocity of the absorption and emission components, 34.0 and 85.8 km s^{-1}, respectively, are in fair agreement with measurements by Pollard et al. for this phase. The photospheric velocity of 58.2 ± 3.2 km s^{-1} is obtained from many metal lines. Pollard et al. (1997) did not measure metal lines.

This star proves to be one of the most Fe poor of our entire collection. The Fe I and Fe II lines give $[\mathrm{Fe/H}] = -2.1$ and the atmospheric parameters listed in Table 2. A full line list is given in Table 3 and a summary of the abundances appears in Table 4.[4] Abundances of individual elements provide solid evidence of a photosphere ravaged by dust-gas separation. Especially striking is the high ratio of [S/Fe] and [Zn/Fe]. Figure 1 presents spectra of AD Aql and AC Her near the Zn I 4810 Å line that show the prominence of the latter line in AD Aql relative to Mn I and Cr II lines. Note that AD Aql was hotter when observed than AC Her and more deficient in Mn and Cr yet the Zn I line is strikingly stronger in AD Aql. Lines of S I (also C I) are also of a remarkable strength for such a Fe-poor star. Abundances based on nine S I and four Zn I lines yield consistent results. The abundances of $[\mathrm{S/H}] = 0.0$ and $[\mathrm{Zn/H}] = -0.1$ imply AD Aql was initially of near-solar metallicity with $[X/\mathrm{Fe}] \simeq 0$ defining the star's initial composition. Oxygen with $[\mathrm{O/H}] = -0.2$ supports this conclusion; the oxygen abundance is derived from the O I λ6158 multiplet. The star is apparently O-rich ($\mathrm{C/O} \leq 1$), so the immediate progenitor was not a carbon star, but, of course, some distortion of the C/O ratio may have occurred as a result of the dust-gas separation.

Abundances of metals are well correlated with their condensation temperatures; Figure 2 shows $[X/\mathrm{H}]$ versus condensation temperature.[5] The implication is that iron and other elements with condensation temperatures near 1500 K have been depleted to about 1% of their original abundance, a very effective cleansing of the photosphere.

TABLE 3

INDIVIDUAL ABUNDANCE RESULTS FOR AD Aql

SPECIES	WAVELENGTH (Å)	LOW EXCITATION POTENTIAL (eV)	log *gf*	1994 AUG 16, 18 W_λ (mÅ)	log *e*
C I.....	4228.312	7.68	−2.36	32.2	8.26
	4269.032	7.68	−2.36	40.3	8.39
	4769.997	7.48	−2.29	40.0	8.16
	4775.877	7.49	−2.15	58.9	8.29
	4817.372	7.48	−2.51	21.9	8.01

NOTE.—Table 3 appears in its entirety in the electronic edition of the Astrophysical Journal.

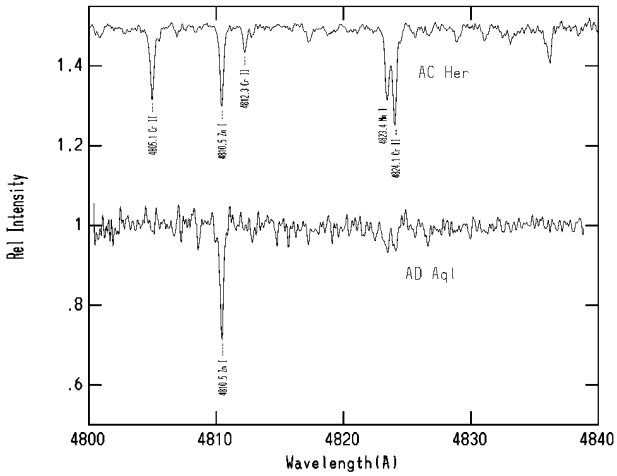

FIG. 1.—Spectra of AC Her and AD Aql near the Zn I line at 4810 Å. Note that the lines of Mn I and Cr II are weak in or absent from the spectrum of AD Aql but that the Zn I line is enhanced.

[2] Usual spectroscopic notation is adopted: $[X/Y] = \log_{10} (X/Y)_{\mathrm{star}} - \log_{10} (X/Y)_{\odot}$.

[3] The convention for RV Tauri variables places phase 0.0 as the deeper minimum, and then the shallower minimum is close to phase 0.5.

[4] Tables 3, 5, 6, 7, and 9 appear in their entirety in the electronic edition of the Astrophysical Journal.

[5] Condensation temperatures are taken from Wasson (1985) and Savage & Sembach (1996). They are the temperature for gas of solar composition at a pressure of 10^{-4} atm, at which 50% of the element has condensed into grains.

TABLE 4

FINAL ABUNDANCES

	AD Aql			DS Aqr			V360 Cyg			AC Her			V453 Oph		
SPECIES	[X/Fe]	[X/H][a]	n	[X/Fe]	[X/H]	n	[X/Fe]	[X/H]	n	[X/Fe]	[X/H]	n	[X/Fe]	[X/H]	n
C I	1.81	−0.31	14	...	...	...	< −1.0	< −2.4	2	1.05	−0.35	10	0.20	−1.94	2
O I	1.88	−0.24	3	0.67	−0.33	3	0.87	−0.53	2	1.18	−0.22	3	0.20	−1.94	1
Na I	1.84	−0.28	4	...	...	...	0.30	−1.10	3	0.62	−0.78	4	...	...	...
Mg I	0.42	−1.70	3	...	...	...	0.35	−1.05	3	0.27	−1.13	7	0.31	−1.85	1
Al I	...	...	1	−0.44	−1.44	2	...	...	...	−1.04	−2.44	1	...	...	...
Si I, II	0.67	−1.45	1	0.16	−0.84	7	0.48	−0.92	4	0.46	−0.94	12	0.47	−1.69	1
S I	2.09	−0.03	9	−0.08	−1.08	2	0.52	−0.88	1	1.03	−0.37	11	...	...	...
K I	1.45	−0.67	1	0.91	−0.09	1	...	...	...	1.17	−0.23	1	...	...	...
Ca I, II	−0.10	−2.22	3	−0.01	−1.01	8	0.14	−1.26	8	−0.10	−1.50	22	0.30	1.86	7
Sc II	0.33	−1.79	2	0.07	−0.93	2	...	...		−0.30	−1.70	10	0.01	−2.15	3
Ti I, II	−0.45	−2.57	4	...	...	...	0.12	−1.28	20	−0.24	−1.64	14	0.41	−1.85	7
V I, II	−0.54	−2.66	1	...	...	...	...	...	...	0.14	−1.26	1	...	...	...
Cr I, II	−0.04	−2.16	12	...	...	...	−0.30	−1.70	12	−0.02	−1.42	33	−0.17	−2.33	1
Mn I	0.84	−1.28	2	...	...	...	−0.35	−1.75	1	0.40	−1.00	7	...	...	...
Fe I, II	...	−2.12	45	...	−1.00	28	...	−1.40	70	...	−1.40	169	...	−2.16	58
Co I	...	...	...	...	...	...	...	...	...	0.50	−0.90	1	...	...	...
Ni I	...	...	...	−0.07	−1.07	6	−0.04	−1.44	4	−0.01	−1.41	25	0.10	−2.06	2
Zn I	2.00	−0.12	4	...	...	...	0.04	−1.36	3	0.47	−0.93	4	...	...	...
Y II	...	...	...	...	...	...	−0.02	−1.42	2	−0.46	−1.86	5	0.33	−1.83	2
Zr II	...	...	...	...	...	...	...	...	...	...	...	...	...	...	...
Ba II	−0.72	−2.94	3	0.91	−0.09	1	0.03	−1.37	5	−0.20	−1.60	3	0.29	−1.87	3
Ce II	...	...	...	...	...	...	...	...	...	−0.19	−1.59	6	...	...	...
Nd II	...	...	...	...	...	...	...	...	...	−0.17	−1.57	3	...	...	...

[a] Solar-meteoritic abundances used to estimate [X/H] are taken from Grevesse, Noels, & Sauval 1996.

Remarkably, AD Aql is a star *without* an infrared excess, implying the current lack of a circumstellar shell!

4.2. *The RV C Star DS Aquarii*

DS Aquarii is a RV C star with the photometric type RVa. Our analysis is based on a single Sandiford echelle spectrogram obtained on 1995 December 11 and covering the wavelength range 6250–8300 Å. A heliocentric velocity of -26.5 ± 0.5 km s^{-1} is obtained. The phase is computed to be 0.80 from the ephemeris given by the General Catalogue of Variable Stars (GCVS; Kukarin et al. 1958; Kholopov et al. 1985). Hα has weak emission wings to a deep central absorption.

Metal lines are few and weak in the spectrum, as expected of a RV C star. The iron lines give [Fe/H] = −1.0 and the atmospheric parameters listed in Table 2. Unfortunately, the observed suite of lines (Table 5) samples few elements. The composition is seemingly close to that expected of a [Fe/H] ∼ −1 unmixed star. Relative abundances of α elements are slightly less than expected: [Si/Fe] = 0.2, [S/Fe] = −0.1, and [Ca/Fe] = 0.0 instead of an expected value of about 0.3 for these elements. Oxygen, based on the O I lines at 7774 Å, has a high relative abundance: [O/Fe] = 0.7. These permitted lines are susceptible to non-LTE effects that strengthen the lines resulting in an overestimate of the LTE abundance estimate. The lines in DS Aqr are not very strong (equivalent widths of 130–160 m Å) so that non-LTE effects are possibly slight. Two remarkable results are the high K ([K/Fe] = 0.5) and Ba ([Ba/Fe] = 0.9) abundances. Both results are based on a single but securely identified line. The Ba II line is somewhat sensitive to the (well determined) microturbulence but [Ba/Fe] ≃ 0 is most unlikely. The Ba overabundance may be the signature of *s*-processing in the star's progenitor. The K abundance is unexplained unless the line is of circumstellar or interstellar origin.

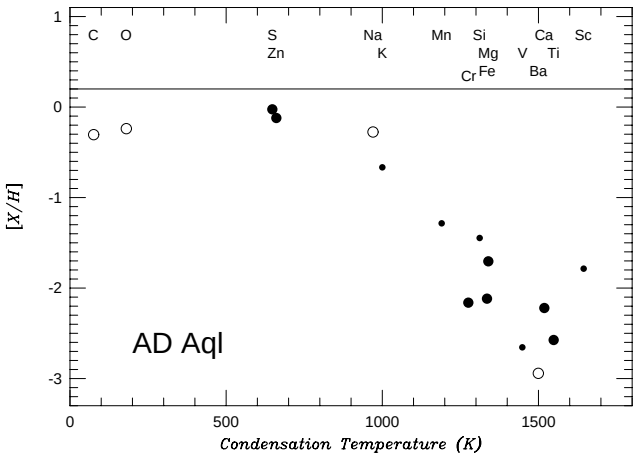

FIG. 2.—Abundance [X/H] vs. condensation temperature for AD Aql. Open symbols denote elements whose abundance is possibly changed by mixing in the red giant phase (C, O. Na, and Ba in order of increasing condensation temperature). Small symbols denote elements whose abundance is determined from not more than two lines.

TABLE 5

INDIVIDUAL ABUNDANCE RESULTS FOR DS Aqr

		LOW EXCITATION		1994 JUN 24	
SPECIES	WAVELENGTH (Å)	POTENTIAL (eV)	log *gf*	W_λ (mÅ)	log ϵ
O I	7771.954	9.14	0.33	165.0	8.58
	7774.164	9.14	0.19	147.0	8.50
	7775.404	9.14	−0.05	130.0	8.55
Al I	7361.290	4.02	−0.55	4.4	5.05
	7361.557	4.02	−0.72	3.0	5.06
Si I	7165.578	5.87	−0.54	25.2	6.72
	7235.328	5.61	−1.36	9.0	6.80

NOTE.—Table 5 appears in its entirety in the electronic edition of the Astrophysical Journal.

Signatures of a dust-gas separation seem to be absent with S and Sc, in particular, showing no obvious anomalies in their abundances relative to Fe. A more detailed analysis is needed with coverage of the blue spectral region permitting measurements of the Zn and additional *s*-process abundances.

4.3. *The RV C Star V360 Cygni*

V360 Cygni has the remarkable radial velocity of -250 km s^{-1} (Joy 1952). Photometrically, the star is a RVa variable. Since the period (70.39 days) given in the GCVS fits photometry by Schmidt & Seth (1996) that was done just a few cycles before our observations, we compute the phases (Table 2) of the latter from minimum light observed by Schmidt & Seth. Both spectra were obtained when the star was near its mean magnitude.

The spectra are characterized by weak metal lines and pronounced emission at Hα. The metal lines confirm the star's high radial velocity: -241.6 ± 0.9 km s^{-1} on 1994 June 25 (phase = 0.25) and -262.2 ± 2.0 km s^{-1} on 1994 September 13 (phase = 0.39). The Hα emission profile is cut by a deep central absorption, which at this phase (0.25) is blueshifted by about 24 km s^{-1} relative to the metal lines. Red and blue emission components are of about the same intensity. Emission at Hβ is similar but weaker. Our detailed abundance analysis is based on the 1994 June "blue" spectra and the 1994 September "red" spectra. Measured lines and corresponding abundances are given in Table 6 and mean abundances in Table 4.

Inspection of Table 4 shows that with minor exceptions V360 Cyg has the expected composition of an unevolved metal-poor star. Of course, V360 Cyg is evolved but composition changes attributable to evolution are minor, at least to the investigated elements. The iron abundance [Fe/H] = -1.4 is not particularly extreme for a Population II star. For the α elements, Mg, Si, and S show the expected enhancement with O showing a more extreme overabundance (relative to Fe). Calcium and Ti are apparently less abundant than expected for metal-poor stars: [α/Fe] $\simeq 0.1$ instead of the usual 0.3. Perhaps, this is indicative of small departures from LTE or very mild effects of dust-gas separation. Sodium is overabundant: [Na/Fe] = 0.3, which may indicate a self-enrichment from deep mixing. Zinc with [Zn/Fe] = 0 has the abundance expected of a metal-poor star (Sneden & Crocker 1988). The *s*-process elements are not enriched: [Y/Fe] $\simeq$ [Ba/Fe] $\simeq 0.0$. Carbon is underabundant; the C I lines near 7115 Å are not present in the spectra and set the limit [C/Fe] ≤ -1.1.

There is no evidence that V360 Cyg is metal-depleted, i.e., a dust-gas separation has not influenced the atmospheric composition. In cases where the separation is effective, the composition is marked by such unusual ratios as [S/Fe] ~ 1.5, [Zn/Fe] ~ 1, and [Sc/Fe] ~ -1. V360 Cyg, however, has [S/Fe] = 0.5, [Zn/Fe] = 0.0, and [Sc/Fe] = 0.2, about as expected for a metal-poor as distinct from a metal-depleted star. The low carbon abundance and the lack of a *s*-process enrichment indicate that V360 Cyg did not evolve through the third dredge-up on the AGB.

4.4. *The RV B Star AC Herculis*

Extensive photometry and spectroscopic studies have been reported for this bright RV B star. AC Her is a RVa variable with a relatively stable period of 75.46 days (Percy, Bezuhly, & Milanowski 1997). Two sets of spectra were analyzed by us. The first spectra were obtained in 1996 April 9–11 with the Sandiford echelle spectrograph in the wavelength intervals 4810–5530 Å and 6400–8600 Å. The second spectrum from the 2.7 m 2dcoudé spectrograph was obtained on 1997 June 20 and covers the interval 3750–11,000 Å but wavelength coverage is incomplete for wavelengths longer than about 5600 Å. Phases of these observations were computed from the deep minimum at JD = 2447341.71 observed by Shenton et al. (1992). A phase of 0.70 is estimated for the 1996 April observations, and of 0.48 for the 1997 June observations. In both series, the absorption lines appear single and symmetric. Radial velocities from many metal lines are -37.9 ± 1.8 km s^{-1} for 1996 April and -20.3 ± 1.4 km s^{-1} for 1997 June. The profile of Hα in 1996 April has two strong emission components separated by deep absorption at a velocity of -31.9 km s^{-1}. In the 1997 June 20 spectrum, Hα shows a P Cygni profile with two absorption components. The line is too close to the edge of the recorded order for reliable measurement of velocities. A P Cygni profile is also seen in the 1997 July 25 spectrum in which the broad (FWHM = 110 km s^{-1}) absorption consists of several components.

The two sets of spectra give similar atmospheric parameters (Table 2): ($T_{\rm eff}$, log g, ξ) = (6000 K, 1.25 cgs, 4.0 km s^{-1}) for 1996 April, and (5800K, 1.0 cgs, 4.2 km s^{-1}) for 1997 June. Table 7 gives the measured lines. Table 8 summarizes the abundances. Mean results are also given in Table 4. Inspection shows that results from the different spectra agree very well. This is gratifying as the Hα profiles are quite different.

Previously published analyses agree quite well with our results. Baird (1981) obtained [Fe/H] $\simeq -1.2$ from a model atmosphere analysis of spectra obtained at several different phases. This is fortuitously close to our result; Baird suggested the error was a factor of 2–3 (i.e., 0.3 to 0.5 dex). He also undertook a curve of growth analysis reporting

TABLE 6

INDIVIDUAL ABUNDANCE RESULTS FOR V360 Cyg

				1994 JUN 25		1994 SEP 13	
SPECIES	WAVELENGTH (Å)	LOW EXCITATION POTENTIAL (eV)	log gf	W_λ (mÅ)	log ϵ	W_λ (Å)	log ϵ
C I	7113.177	8.64	-0.92	...	...	10.0	6.05
	7116.927	8.65	-1.08	...	...	11.0	6.25
O I	6300.437	0.00	-9.75	...	...	30.0	8.28
	6363.887	0.00	-10.25	...	...	15.0	8.41
Na I.....	4668.577	2.10	-1.25	15.0	5.28	...	...

NOTE.—Table 6 appears in its entirety in the electronic edition of the Astrophysical Journal.

TABLE 7

INDIVIDUAL ABUNDANCE RESULTS FOR AC Her

SPECIES	WAVELENGTH (Å)	LOW EXCITATION POTENTIAL (eV)	log *gf*	1996 APR 9–11 W_λ (mÅ)	1996 APR 9–11 log ϵ	1997 JUN W_λ (Å)	1997 JUN log ϵ
C I.....	4770.00	7.48	−2.29	...	...	56.7	8.44
	4775.88	7.49	−2.15	...	...	53.9	8.27
	4817.38	7.48	−2.51	24.2	8.12	...	...
	4932.07	7.68	−1.78	60.0	8.16	...	...
	5380.32	7.68	−1.76	64.9	8.23	63.5	8.20

NOTE.—Table 7 appears in its entirety in the electronic edition of the Astrophysical Journal.

without details that all elements excluding C, N, and O were as underabundant as Fe ([*X*/Fe] ~ 0) "with the possible exception of Co, Zn, and Sr." The overabundance of Co and Zn is confirmed here. Strontium was not among our sample of elements. The Borisov & Panchuk (1986) model atmosphere analysis gave [Fe/H] = −1.25. Relative abundances [*X*/Fe] of six elements show large differences with our results, e.g., [Ni/Fe] = 1.3 but 0.0 according to us. Yoshioka (1979) from a curve of growth analysis with checks via ϵ Vir (G8 III) and 35 Cyg (F5 Ib) obtained [Fe/H] = −1.2, also in fair agreement with our result. Relative abundances [*X*/Fe] were provided by Yoshioka for 14 elements from atomic lines and for C and N from molecular (CH and CN) lines. For the former 14 elements, the difference in [*X*/Fe] between our analysis and Yoshioka's is 0.0 ± 0.3. If one extreme difference (vanadium) is excluded, the mean is -0.1 ± 0.2. This is remarkably good agreement.

Examination of Table 4 shows that S and Zn have subsolar abundances but that elements with higher condensation temperatures, such as Al, Ca, and Fe, are much more severely underabundant. This difference is the signature of the dust-gas separation. If S and Zn are unaffected by the separation, they indicate that AC Her's progenitor was initially metal poor with [Fe/H] ≃ −0.7. In Figure 3, we show the abundances [*X*/H] measured not with respect to the Sun but to a typical metal-poor star with [Fe/H] = −0.7 whose composition is taken from the Lambert (1989) review of metal-poor stars. There is a clear correlation between the abundances and the condensation temperatures. Carbon appears to be overabundant by about 0.3 dex. The *s*-process elements have the abundances anticipated by the abundance-condensation temperature plot, i.e., the star is not enriched in *s*-process products.

In evolution from the main sequence to the RV Tauri stage, the abundance of certain elements will be altered as products from H-burning and He-burning regions are mixed to the surface. Carbon certainly seems to have been increased. Oxygen is expected to be little affected by these dredge-ups, as is observed. If the third dredge-up is responsible for the carbon enhancement, it obviously did not increase the abundances of the *s*-process elements.

In summary, the abundance analysis shows that AC Her has a photosphere affected by the dust-gas separation, and, if, as seems indicated by the carbon abundance, the star evolved to the AGB, it evolved off before the third dredge-up enriched the atmosphere in products of the *s*-process.

TABLE 8

INDIVIDUAL ABUNDANCES FOR AC Her

SPECIES	1996 APR 9–11 [*X*/H]	*n*	1997 JUN 20 [*X*/H]	*n*	MEAN [*X*/H]	MEAN [*X*/Fe]
C I	−0.36	10	−0.34	10	−0.35	1.05
O I	...	...	−0.22	3	−0.22	1.18
Na I	...	...	−0.78	4	−0.78	0.62
Mg I	−1.39	1	−1.13	6	−1.13	0.27
Al I	−2.44	1	...	...	−2.44	−1.04
Si I	−0.93	5	−0.94	7	−0.94	0.46
S I.....	−0.33	4	−0.42	7	−0.37	1.03
K I	−0.23	1	...	...	−0.23	1.17
Ca I	−1.40	7	−1.56	13	−1.48	−0.08
Ca II	−1.39	1	−1.61	1	−1.45	−0.05
Sc II.....	−1.84	2	−1.67	8	−1.70	−0.30
Ti I	−1.95	1	...	...	...	...
Ti II.....	−1.93	2	−1.63	12	−1.64	−0.24
V II	...	...	−1.26	1	−1.26	0.14
Cr I	−1.55	3	−1.44	10	−1.47	−0.07
Cr II	−1.46	7	−1.34	14	−1.38	0.02
Mn I	−0.94	1	−1.01	6	−1.00	0.40
Fe I	−1.44	52	−1.38	82	−1.41	...
Fe II	−1.45	9	−1.37	26	−1.39	...
Co I.....	...	...	−0.90	1	−0.90	0.50
Ni I	−1.43	12	−1.39	13	−1.41	−0.01
Zn I.....	−0.91	1	−0.91	3	−0.93	0.47
Y II	...	...	−1.86	5	−1.86	−0.46
Ba II	...	...	−1.60	3	−1.60	−0.20
Ce II	...	...	−1.59	6	−1.59	−0.19
Nd II.....	...	...	−1.57	3	−1.57	−0.17

4.5. *The RV C Star V453 Oph*

This RV C star of photometric type RVa was observed in 1994 August with the Sandiford spectrograph. According to

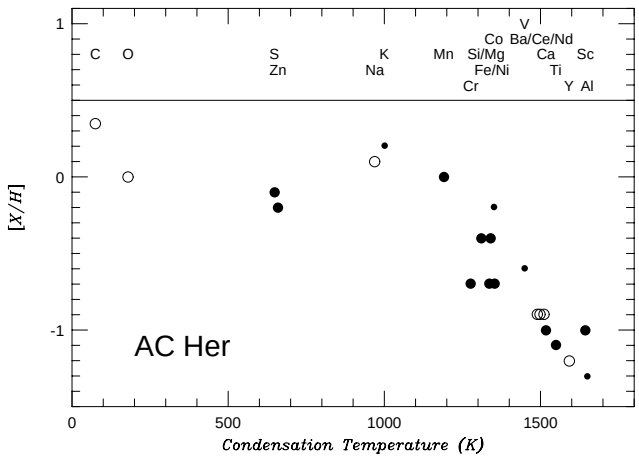

FIG. 3.—Abundance [*X*/H] vs. condensation temperature for AC Her. As described in the text, [*X*/H] is not the directly measured abundance but is adjusted to a reference star having [Fe/H] = −0.7. Symbols have the same meanings as in Fig. 2.

Pollard's ephemeris (K. R. Pollard 1998, private communication), observations were made at phase 0.82. Spectra covering the intervals 4870–5620 Å and 5750–8200 Å were obtained. Inspection confirms the designation RV C. Our radial velocity of -118.6 ± 1.2 km s^{-1} from metal lines also indicates membership of Population II. Hα shows strong blue and red emission separated by a deep absorption at a radial velocity of -119.7 km s^{-1}. This velocity (and profile) is similar to that reported by Pollard et al. (1997) for phases of 0.41 (-119.2 km s^{-1}) and 0.76 (-125.2 km s^{-1}).

The iron lines give [Fe/H] = -2.2 and the atmospheric parameters listed in Table 2. The line list (Table 9) gives the mean abundances listed in Table 4. At this metallicity, unevolved stars are enriched in the α elements by about 0.4 dex relative to Fe. This is strikingly true too of V453 Oph: [X/Fe] = 0.3, 0.5, 0.3, and 0.4 for Mg, Si, Ca, and Ti respectively. One weak line of O I at 6158 Å gives [O/Fe] = 0.2. This degree of uniformity is in contrast to the results for DS Aqr and V360 Cyg where Ca and Ti appeared less abundant than expected (see also our analyses of the two metal-poor SRd variables AB Leo and SV UMa [Giridhar, Lambert, & Gonzalez 1998]). Perhaps, there is a real difference in the Ca/Fe and Ti/Fe ratios among these RV C stars. The s-process elements are nominally overabundant: [s/Fe] = 0.3 from Y and Ba. If these abundances are considered relative to their abundances in a metal-poor star of [Fe/H] = -2.2 (i.e., [Y/Fe] $\simeq -0.3$ and [Ba/Fe] = -0.5 according to Spite & Spite 1978), Y and Ba are overabundant in V453 Oph by about 0.6 and 0.8 dex respectively. This is a significant s-process enrichment. Carbon may be slightly overabundant: weak C I lines at 5052 Å and 5380 Å give [C/H] = -1.9 or [C/Fe] = 0.2.

Lacking the crucial S and Zn abundances, a decisive ruling on whether V453 Oph is affected by dust-gas separation cannot be given. The fact, however, that Ca, Sc, and Ti (relative to Fe) have normal abundances is suggestive that the separation has not affected the present photosphere. There is evidence that V453 Oph has experienced the third dredge-up or is an evolved Barium (mass-transfer binary) star.

4.6. *Spectrophotometric and Photometric Abundances*

It is of interest to compare the spectroscopic Fe abundances obtained in this series of papers with published values from spectrophotometry by Cardelli (1989) and Wahlgren (1992) and from DDO photometry by Dawson (1979). As we show, the spectrophotometric values differ by a small zero point in [Fe/H] from our spectroscopic values.

TABLE 9

INDIVIDUAL ABUNDANCE RESULTS FOR V453

Species	Wavelength (Å)	Low Excitation Potential (eV)	log gf	1994 Aug 16, 18 W_λ (mÅ)	log ϵ
C I.....	5380.322	7.68	−1.76	4.1	6.64
	5052.151	7.68	−1.51	5.9	6.55
O I	6158.170	10.74	0.29	2.6	6.93
Mg I.....	5528.418	4.34	−0.34	75.0	5.73
Si II.....	6371.360	8.12	−0.05	20.0	5.87
Ca I	5581.979	2.52	−0.88	14.2	5.00

NOTE.—Table 9 appears in its entirety in the electronic edition of the Astrophysical Journal.

A similar conclusion follows from the DDO photometry. After correction, the larger sample of stars considered by Wahlgren and Dawson could be used in searches for correlations between [Fe/H] and, for example, observed infrared excesses.

Our survey has seven stars in common with Wahlgren who derived [Fe/H] from calibrated spectra at a resolution of 2.5 Å fitted with synthetic spectra. The differences $[Fe/H]_{Us} - [Fe/H]_{Wahl}$ range from 0.0 to -0.6 for a mean of -0.3 ± 0.2 over the range $[Fe/H]_{Us}$ from -0.5 to -1.8. This comparison indicates that, apart from a zero-point shift of 0.3 dex, the two techniques yield consistent results.

Cardelli (1989) used spectrophotometric scans to define several indices including one measuring the Ca II H and K lines. His small sample has three stars in common with us. His results for [Fe/H] share with Wahlgren's the fact they are consistently higher than ours. For AC Her, Cardelli obtained [Fe/H] = -1.1 against our -1.4. For EP Lyr, [Fe/H] = -1.6 according to Cardelli but we find -1.8. The difference is larger for V453 Oph, [Fe/H] = -1.6 (Cardelli) and -2.15 (Table 2). A zero-point difference of 0.3 dex is suggested from this small sample.

DDO photometry was used by Dawson (1979) to estimate [Fe/H] from the index C(41–42). His [Fe/H] are systematically larger than ours: six stars comprising three field RV Tauri variables, the two SRd's (Giridhar et al. 1998), and the variable V11 in M2 (Gonzalez & Lambert 1997) give a mean difference $[Fe/H]_{Us} - [Fe/H]_{DDO} = -0.3 \pm 0.2$, the same value as results from the comparison with Wahlgren's estimates of [Fe/H]. One remarkable exception not included in the sample of six is the metal-depleted star V453 Oph with DDO photometry giving [Fe/H] = -0.77, but our spectroscopic result is -2.15. One conjecture is that the DDO photometry measures in part molecular absorption from CN and CH. Our scanty evidence indicates that C and N are appreciably less deficient than indicated by the metal lines and, hence, one expects DDO photometry to provide a systematically higher [Fe/H] estimate.

5. THE DUST-GAS SEPARATION

5.1. *The RV A, B, and C Stars*

One result of our analyses is that stars of intrinsically low metallicity do not exhibit the abundance anomalies that we ascribe to the dust-gas separation. This is clearly the case for V360 Cyg, DS Aqr, likely the case for V453 Oph, and is also the case for the RV Tauri–like variables in globular clusters (Gonzalez & Lambert 1997; Russell 1997). The variable V1 in the globular cluster ω Cen is mildly affected. A detailed abundance analysis by Gonzalez & Wallerstein (1994) of this variable suggests, on the basis of the S and Zn abundances that the initial metallicity of the star was [Fe/H] $\simeq -1.3$. Relative to the composition expected of a star with this iron abundance, underabundances correlate quite well with the predicted condensation temperatures.[6] In the present small samples of RV C and globular cluster stars, the metallicities of stars unaffected by dust-gas separation range up to [Fe/H] $\simeq -1$.

[6] The star is enriched in the heavy elements by about 0.6 dex relative to iron-group elements having the same condensation temperature. Oddly, the enriched elements include Eu to which the s-process is expected to make little contribution. Rubidium is overabundant by 1.6 dex, suggesting that the s-process operated at a high neutron density.

TABLE 10

OBSERVED AND INFERRED PROPERTIES

STAR	TYPE[a]		P[b]	ABUNDANCES					
	Spectroscopic	Photometric	(days)	[Fe/H]	$[Fe/H]_0$	[S/H]	[Zn/H]	[C/H]	[s/X]
DY Aql	A	?	131.4	−1.0	...	...	...	...	...
SS Gem	A	a	89.3	−0.9	−0.2	−0.4	0.0	−0.6	0.5:
R Sge	A	b	70.8	−0.5	0.1	0.4	−0.2	−0.4	0.0
CE Vir	A	?	67:	−1.2	−0.7	...	−0.7	...	0.0
AD Aql	B	a	66.1	−2.1	−0.1	0.0	−0.1	−0.3	−0.3
IW Car	B	b	72.0	−1.1	0.2	0.4	−0.1	0.3	0.0
AC Her	B	a	75.0	−1.4	−0.7	−0.4	−0.9	−0.4	0.0
EP Lyr	B	a	83.3	−1.8	−0.7	−0.6	−0.7	−0.3	0.0
CT Ori	B	?	135.5	−1.9	−0.6	−0.5	−0.6	−0.7	0.2:
DY Ori	B	?	60.3	−2.3	0.2	0.2	0.2	−0.2	1.0
AR Pup	B	b	77.8	−0.9	0.2	0.4	...	0.1	1.3
DS Aqr	C	a	78.2	−1.0	−0.8	−1.1	...	...	0.9
V360 Cyg	C	a	70.4	−1.4	−1.3	−0.9	−1.4	< −2.4	0.0
V453 Oph	C	a	81.3	−2.2	−2.2	...	...	−1.9	0.7

[a] From GCVS, Preston et al. 1963, Lloyd Evans 1985, and Fokin 1994.
[b] From GCVS and Pollard et al. 1996, 1997.

A second result is that, although the effects of the dust-gas separation are present in both RV A and RV B stars, there is a difference between the two groups in the run of the abundances versus condensation temperature. Here, we compare the observed [Fe/H] and [Sc/H] against the iron abundance inferred from the observed S and Zn abundances on the assumption that these elements have not been depleted at all. In calculating this initial iron abundance, we allow for the slight increase of [S/H] and the very slight decrease of [Zn/H] with decreasing [Fe/H] of unevolved stars (Lambert 1989; Sneden & Crocker 1988). We refer to this iron abundance, $[Fe/H]_0$, as the initial abundance (Table 10). These run from 0.2 to −2.2.[7,8] Figure 4 shows that the most extreme iron depletions, $[Fe/H] - [Fe/H]_0$, are found RV B rather than for RV A stars. Among the RV B stars, the severest depletions are found for the two stars with the shortest periods (Table 10). Additional observations will be needed to confirm a correlation between period and metal depletion. The present sample is small but there are no obvious differences in depletions for RV a and RV b of a given spectroscopic class. The distinction between RV A and RV B stars is *not* seen in a comparison of the [Sc/H] depletions, also in Figure 4: Sc and other elements with high condensation temperatures are depleted to similar levels in both classes but elements (e.g., Fe) of a little lower condensation temperature are appreciably depleted only in the RV B stars. Judged by spectral type and color, the RV B stars have higher effective temperatures than the RV A stars and, therefore, are presumed to have shallower convective envelopes. Thus, a dust-gas separation can more easily maintain larger abundance anomalies in the photosphere of a RV B star. Significantly, the RV C stars have similar effective temperatures to the RV B stars so that the lack of dust-gas separation in the RV C stars cannot likely be attributed to a deep convective envelope.

A third important result is apparent from Figure 4. The initial iron abundances of metal-depleted stars are all in excess of $[Fe/H]_0 \geq -1$. Stars less iron rich including the globular cluster variables are unaffected by the dust-gas separation. This suggests that $[Fe/H] \sim -1$ is a minimum abundance needed to drive a dust-gas separation. It is quite possibly significant that the sulphur abundance of the

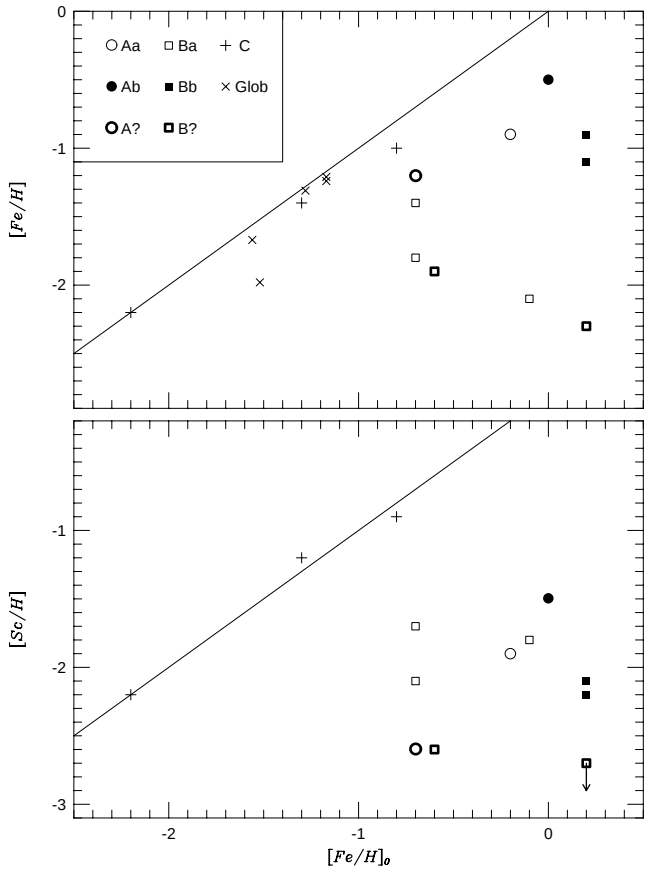

FIG. 4.—Comparisons of the measured [Fe/H] and [Sc/H] against the inferred initial abundance $[Fe/H]_0$. Different types of RV Tauri variables including those in globular clusters are represented by different symbols—see key on the figure.

[7] The mean [S/H] values are −0.1 and 0.0 from 2 RV A and 7 RV B stars, respectively. The mean [Fe/H] values are -0.9 ± 0.3 and -1.6 ± 0.5 from 4 RV A and 7 RV B stars, respectively.

[8] An estimate $[Fe/H]_0 = 0.2$ seems unexpectedly high. While it is possible that systematic errors have led to slight overestimates of $[Fe/H]_0$, it might be remembered that an overlooked hydrogen deficiency would lead to an overestimate of the metallicity.

extremely metal-depleted post-AGB stars implies a $[Fe/H]_0$ close to or in excess of the above limit. For example, data for five stars are summarized by Waelkens et al. (1992) and [S/H] is in the range -0.1 to -1.1 for stars with [Fe/H] of -1.6 to -4.8. The lowest value of [S/H], if unaffected by gas-dust separation, implies $[Fe/H]_0 \simeq -1.4$, a little less than our empirical limit. It is tempting to suggest these post-AGB stars may have evolved from the RV Tauri stars with continuing operation of the dust-gas separation. There are, however, post-AGB stars with metallicities that seem close to the initial values (Van Winckel 1997). These stars either avoided a phase of dust-gas separation or effects present at an earlier stage of evolution have been erased by mixing with the interior.

5.2. *Dust-Gas Separation and Infrared Excess*

An expectation that present infrared excesses should be correlated with the severity of the abundance anomalies attributed to a dust-gas separation is founded on three major assumptions. First, the site of dust-gas separation is assumed to be the wind off the star. The observation that the extremely metal-poor post-AGB stars are spectroscopic binaries implies that the dust-gas separation may occur not in the stellar atmosphere but in the circumbinary environment. An RV Tauri variable in a binary may benefit from this location but, it seems unlikely that all RV Tauri stars belong to binary systems. Second, it is assumed that the dusty stellar wind has blown unchanged since the anomalies were established. Third, there is the assumption that the wind is spherically symmetric. A wind that is not spherically symmetric provides an infrared excess that is dependent on the viewing angle, for example, a dusty torus viewed along the poles with a direct and largely unobscured view of the central star will have a lower infrared excess than the same torus viewed in an equatorial direction in which the star may not be visible.

Infrared excesses of RV Tauri variables have been investigated observationally from ground-based narrow-band photometry from 2 to 11 μm and from *IRAS* measurements. For some stars, the infrared excess is detectable from short wavelengths (J, H, and K photometry) and in other cases longer wavelength observations are needed to detect an excess. These differences reflect the radial distribution of the dust: dust near the star is warm and emits at short infrared wavelengths but dust far from the star is cool and emits at long wavelengths. In turn, radial distribution of dust is likely to reflect the past history of mass loss by the RV Tauri star. Jura (1986) estimates that the coolest dust detected by *IRAS* was ejected about 500 yr ago. From the relative weakness or absence of a near infrared excess, Alcolea & Bujarrabal (1991) argue that mass loss ceased about 100 yr before the RV Tauri phase and that most RV Tauri stars spend about 200 yr in this phase—but see Fokin (1994).

Extensive discussions of $JHKL$ photometry of RV Tauri variables have been provided by Lloyd Evans (1985) and Goldsmith et al. (1987). Infrared excesses are detected through a star's location in a two-color diagram (J-H vs. H-K, and J-K vs. K-L) relative to the location of normal G-M giants. These papers provide adequate data on 11 of the 14 stars examined in this series of papers. ($JHKL$ photometry is seemingly unavailable for V360 Cyg, EP Lyr, and CE Vir.) Infrared excesses range from pronounced for AR Pup and IW Car to undetectable for DY Aql, DS Aqr, SS Gem, and V453 Oph. There is no correlation between an infrared excess, as defined by $JHKL$ photometry, and the severity of the dust-gas separation.

Photometry at longer wavelengths may provide evidence of cooler dust. Infrared excesses of RV Tauri variables were investigated initially by Gehrz (1972) and Gehrz & Ney (1972) through photometry from 2.2 to 22 μm. Few stars were measured at wavelengths longer than 11.3 μm, and the color index [3.6]$-$[11.3] was the principal measure of an infrared excess. (As Lloyd Evans 1985 has noted, this index is not a true measure of the excess flux at 11 μm from dust because the 3.6 μm flux in many cases is not purely photospheric radiation but receives a contribution from dust.) Unfortunately, several stars in our sample were not observed by Gehrz and observations at about 11 μm appear not to have been made subsequently. *IRAS* observations at 12 μm are available for several of our stars including two (CT Ori and DT Ori) for which the [11.3] magnitude is unavailable. By establishing the calibration between the [11.3] magnitudes and *IRAS* 12 μm fluxes from stars for which both measures are available, we estimate [11.3] magnitudes for CT Ori and DT Ori. Then, the color index [3.6] $-$ [11.3] is available for a majority of the stars listed in Table 7. There is no evidence from our small sample that the color index is correlated with the depletion index D.

A correlation between the [3.6] $-$ [11.3] color and metallicity was claimed by Dawson (1979) for RV A and RV C stars following a suggestion by Gehrz (1972) that the infrared excess was higher for the RV A than for RV C stars. Dawson's Figure 7 is redrawn in Figure 5 using corrected DDO [Fe/H] estimates and colors from Gehrz. Apart from the 0.3 dex reduction to [Fe/H], this plot should be identical to that presented by Dawson. There are minor differences: a couple of Dawson's data points appear not to correspond to stars observed by him, and his figure failed to distinguish between measured color indices and upper limits. Dawson's suggested linear fit to the data corresponds to [3.6] $-$ [11.3] = 3.9 + 1.1[Fe/H] where [Fe/H] is now the corrected DDO [Fe/H]. His plot did not include the lone RV B (AC Her) star observed by him, which, despite the lack of a DDO [Fe/H] estimate, could be seen not to

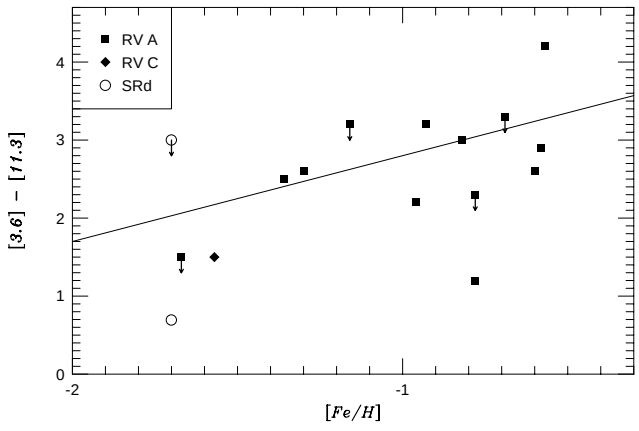

FIG. 5.—Color index [3.6] $-$ [11.3] vs. [Fe/H] for stars observed photometrically by Dawson (1979) with color indices from Gehrz (1972). The photometric [Fe/H] has been reduced by 0.3 dex (see text). RV A, C and SRd variables are plotted—see key on the figure. The line denotes Dawson's suggested fit, as adjusted to account for the 0.3 dex correction to the photometric [Fe/H].

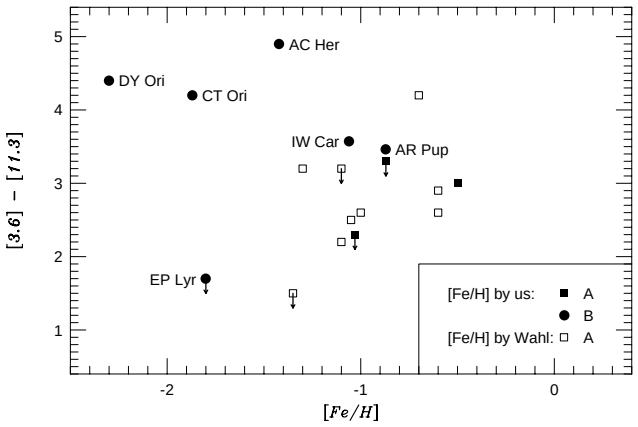

FIG. 6.—Color index [3.6] − [11.3] vs. [Fe/H] for stars with [Fe/H] from our analyses (*filled symbols*) and [Fe/H] from Wahlgren (1992) after correction by −0.3 dex (*open symbols*). Note the extraordinary location of the RV B stars DY Ori, CT Ori, and AC Her.

follow the "trend": [3.6] − [11.3] = +4.9 for AC Her.[9] In Figure 6, we show [3.6] − [11.3] versus [Fe/H] for our stars, and for additional stars observed by Wahlgren (1992). The body of the data points mimic Dawson's sample, as expected because the [Fe/H] estimates are identical in the mean and the color indices are from a common source. Our sample does not yet contain an adequate number of RV A stars of low [Fe/H] to confirm Dawson's correlation between infrared excess and metallicity.[10]

Nonetheless, three stars seem to possess an extraordinary infrared excess for their metallicity. Two of the three (DY Ori and CT Ori) are greatly affected by dust-gas separation but the third (AC Her) is only slightly affected. All three are RV B stars but EP Lyr, a RV B of similar [Fe/H] to CT Ori, has the low infrared excess expected of Dawson's correlation. There is no obvious compositional difference that can account for the location of EP Lyr in Figure 6. EP Lyr's seemingly anomalous position in the figure would be normal if it were a RV A rather than a RV B star but the classification RV B was assigned by Preston et al. (1963) who introduced the classification scheme.

Separation of RV A from RV B stars is similarly found from the *IRAS* 12, 25, 60, and 100 μm flux densities (Raveendran 1989). *IRAS* detections are available for 16 RV Tauri variables. In the [25] − [60] versus [12] − [25] diagram, the RV A and RV B stars define abutting domains. Raveendran shows that the RV B stars have cooler shells: if T_0 is the temperature of the shell's inner boundary where gas condenses into grains, the RV A–RV B divide is at $T_0 \simeq 460$ K. There is no obvious connection between T_0 and the severity of the dust-gas separation. Six of our stars have *IRAS* measurements. The two stars with the coolest T_0 according to Raveendran are AC Her ($T_0 = 260$ K) and DY Ori ($T_0 = 295$ K). DY Ori is severely affected by dust-gas separation but AC Her is but mildly affected. Four stars quite similarly affected span almost the entire range of T_0.

[9] Dawson expressed the opinion that the class RV B is "a dumping ground" for a few variables not fitting into either the RV A or RV C classes. Our finding that the most metal-depleted stars are RV B stars imply that the class is distinct from the other classes.

[10] A similar correlation is found for AGB stars in the Galaxy, the LMC ([Fe/H] $\simeq -0.3$), and the SMC ([Fe/H] $\simeq -0.7$): the dust optical depths of LMC and SMC stars are about 70% and 7%, respectively, those of Galactic stars (Groenewegen et al. 1995).

Jura (1986) argued that the wavelength distribution of the infrared excess (i.e., the radial distribution of dust) implies that RV Tauri variables have just ended a phase of high mass loss. Raveendran disputes this conclusion. It is interesting that Jura's estimates of the rate of mass lost as dust show the RV B stars to have on average higher rates: the mean rate from the 8 RV A stars is 4.7×10^{17} g s^{-1} from a range of (0.17–13) $\times 10^{17}$ g s^{-1} and the mean from 9 RV B is 11×10^{17} g s^{-1} from a range of (1.2–40) $\times 10^{17}$ g s^{-1}. Within the RV B sample, there is no correlation between the mass loss rate of dust and the depletion introduced by dust-gas separation.

5.3. *Is Condensation Temperature THE Controlling Influence?*

Our assertion that a dust-gas separation affects the RV Tauri variables is based in large part on the correlation of the abundance anomalies with the predicted condensation temperatures and, as shown explicitly for IW Car (Giridhar et al. 1994), with the observed depletions for diffuse interstellar gas along the line of sight to ζ Oph. Although the infrared excesses do not correlate in detail with the effects of the dust-gas separation, there is a general correlation. There remains the prospect that other atomic properties control the abundance anomalies that appear correlated with condensation temperature because it is correlated with the true controlling atomic property. Ionization potential of the neutral atom is an obvious alternative to the condensation temperature. In this case, the conjecture is that singly charged ions in the photosphere are more easily fed into the stellar (gas) wind that may be driven by radiation pressure on dust grains. If the mass loss by gas exceeds that by dust, the first ionization potential (here, FIP) may be the controlling factor on the photospheric composition. Figure 7 shows the abundance anomalies of AD Aql plotted versus the FIP. The correlation is marred by the alkalis Na and K—and Al for those stars in which it is measured. We conclude that the FIP is not a controlling factor. The alkalis fit more smoothly into a plot that uses the ionization potentials of the singly charged ions but this plot exhibits more scatter than plots against condensation temperature. Luck & Bond (1989) in seeking to explain their observations of heavy element underabundances in low mass supergiants such as RV Tauri variables (e.g., RU Cen and U Mon) suggest that Lyman continuum emission from shock waves

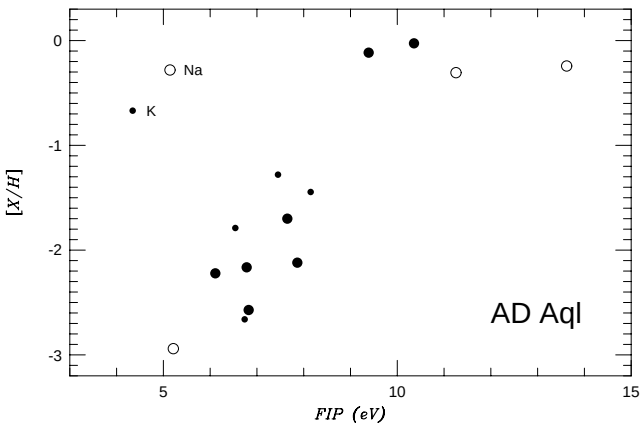

FIG. 7.—Abundance [X/H] vs. the ionization potential of the neutral atom (FIP). Symbols have the meanings expressed in Fig. 2. Note the location of the points representing the alkali atoms K and Na.

may result in overionization of elements with second ionization potentials less than that of hydrogen.[11] This cannot account for the underabundances observed for AD Aql and our other stars because marked underabundances are found for elements with second ionization potentials greater than 13.6 eV, e.g., Si, V, Cr, Mn, and Fe. Unfortunately, Luck & Bond's analysis of RU Cen, and U Mon did not include S and Zn so that it is difficult to assess the role of dust-gas separation but we suppose it might be substantial.

A curious puzzle is provided by the Luck (1981) analysis of R Sct, which also omitted S and Zn but yielded the remarkable result that *s*-process elements were underabundant by large factors ([Ba/Fe] = −0.5 to [Pr/Fe] = −1.7) that cannot be easily attributed to a dust-gas separation; Ca and Ti with condensation temperatures similar to those of the *s*-process elements were not correspondingly underabundant ([Ca/Fe] ≃ [Ti/Fe] ≃ −0.2). Luck supposed that the atmosphere was substantially enriched in helium and these low *s*-process abundances were reflective of a much lower initial [Fe/H] (Spite & Spite 1978). Assumption of a normal He/H ratio in the analysis does not materially affect the derived Ba/Fe ratio, for example, but results in a spuriously high [Fe/H]. R Sge (Gonzalez et al. 1997a) appears quite similar to R Sct with [Y/Fe] = −1.2 and [Ba/Fe] = −1.4. However, unlike R Sct, R Sge has low abundances of other elements with condensation temperatures similar to those of the *s*-process elements. Thus, R Sge's *s*-process abundances are not unusual in light of a dust-gas separation limited to elements of the highest condensation temperatures. As we noted above, this is a characteristic of RV A stars. Pending a reexamination of R Sct, we are hesitant to invoke drastic scenarios such as severe hydrogen deficiency.

5.4. *The Progenitors of the RV Tauri Variables*

Evolution prior to the RV Tauri phase may have marked the photospheric compositions; for example, evolution along the AGB and experience of the third dredge-up will most likely have led to enrichment of the photosphere in carbon and the *s*-process elements. On the other hand, if RV Tauri variables evolve from either He-core burning giants or the early phases of the AGB, a carbon deficiency, the fruits of the first dredge-up, and normal *s*-process abundances are likely to be expected. In relating the observed compositions to these expectations, the effects of the dust-gas separation have to be considered. In particular, abundances should be referred to the estimated initial metallicity, $[Fe/H]_0$, and corrected empirically for deficiencies induced by the dust-gas separation processes.

Table 10 summarizes the photometric and abundance data on RV Tauri variables analyzed by us. With its low condensation temperature, the directly measured [C/H] may be compared with the presumed initial abundance computed from $[Fe/H]_0$ and [C/Fe] = 0. The observed [C/Fe] computed from $[Fe/H]_0$ range from +0.3 (AC Her and EP Lyr) to −0.5 (R Sge) for a mean of -0.1 ± 0.3 for nine RV A and RV B stars. Since this estimate exceeds slightly the [C/Fe] for giants that have undergone the first dredge-up, the [C/Fe] of the RV Tauri variables is weak evidence for carbon enrichment.

To assess *s*-process enrichment, the observed abundances must be adjusted for effects of dust-gas separation. This is done by examining the positions of *s*-process elements in the $[X/H]$ versus condensation temperature plots such as Figures 2 and 3. Comparison of $[X/H]$ for *s*-process elements and lighter elements of similar condensation temperature gives the $[s/X]$ estimates in Table 10. A minority of the stars show clear *s*-process enrichment: AR Pup, V453 Oph, DY Ori, and DS Aqr. One other—SS Gem—may be mildly enriched. A majority have quite normal abundances ($[s/X] \simeq 0$) of the *s*-process elements.

The conclusion must be that the RV Tauri variables, in general, are not descended from AGB giants that have experienced the third dredge-up. Those that are *s*-process enriched may have evolved from the AGB or achieved that enrichment at an earlier stage from a companion that evolved to the AGB and is now present as a white dwarf.

6. CONCLUDING REMARKS

Abundance analyses reported in this and earlier papers of the series suggest several novel conclusions. Most importantly, the photospheres of the RV Tauri variables have been cleansed of those elements that condense into grains in circumstellar environments. This separation of dust from gas is most severe for the RV B stars but is present also in the RV A stars. The RV C stars including their globular cluster counterparts are not so affected. Although one may see in this distinction a metallicity dependence on the efficiency of the dust-gas separation, it is not a simple dependence on the present [Fe/H] of the atmosphere; some of the stars unaffected by the dust-gas separation have higher Fe abundances than the RV A and B stars in which separation has been serious. What does seem to be an important factor is the initial metallicity. As Figure 4 suggests, stars with an initial metallicity $[Fe/H]_0 \geq -0.8$ are prone to the effects of dust-gas separation but more metal-poor stars are not.

Our assumption is that the dust-gas separation occurs in the upper atmosphere of the RV Tauri variable. As the case of AD Aql suggests with its severe effects of dust-gas separation but no infrared excess, separation may not be a continuous process. (We recognize that alternative venues for separation are possible, i.e., a circumbinary envelope as suggested for the post-AGB stars.) Separation may be considered to involve several steps in each of which metallicity may play a role: (1) gas must be cooled to lower temperatures at which grain condensation may begin, (2) condensation into grains occurs, (3) grains are driven out by radiation pressure, and (4) gas cleansed to some degree of condensable elements falls back to the photosphere. Step 1 is dependent on the composition of the subphotospheric layers that are likely to be the composition of the star unaffected by the dust-gas separation. If the pulsation amplitudes decrease with initial metallicity such that little gas is pushed to high altitudes, the difference between RV C and the RV A+B stars could be explained. The effect of a dust-gas separation on photospheric abundances depends also on the degree of mixing from below the photosphere of gas with an unmodified composition. The time available for grain condensation is limited to a fraction of the pulsational period. At low metallicity, it obviously takes longer to grow a grain by collisions between it and metal atoms, and at some metallicity grain formation is effectively impossible

[11] An underabundance of *s*-process elements relative to iron may be a consequence of dust-gas separation, as is shown by Figure 2. If the *s*-process abundances are compared with those of lighter elements of the same condensation temperature, an apparent underabundance may vanish.

between the time the gas is pushed up and the time it falls back. Finally, grains driven out by radiation pressure experience the drag from the circumstellar gas atoms and molecules. Grains formed at low metallicity experience a higher drag than grains formed at high metallicity. In short, the initial metallicity may well play a role in setting the efficiency of the dust-gas separation, and the separation may saturate once the metallicity has been reduced to a low critical value. For the RV B Tauri stars, that low metallicity appears to be [Fe/H] ~ -2.3. The critical metallicity is higher ([Fe/H] ~ -1) for RV C stars. Post-AGB stars may achieve a much lower metallicity, [Fe/H] ~ -4 to -5, suggesting that either the efficiency is higher for these more evolved stars or the process operates in a different locale (e.g., a circumbinary disk).

Theoretical examination of the above speculative scenario is welcome. Additional insights are likely to come from continued pursuit of RV Tauri variables. Many with severe infrared excesses have yet to be analyzed. By careful spectroscopy of stars with dusty circumstellar shells, it may be possible to map the gas flows up and down and to see dust-gas separation occurring in real time. If the critical episode of dust-gas separation occurs each pulsation following a burst of grain formation, it may be possible to detect grain formation through an increase in the near-infrared flux or by polarimetry thanks to light scattered by the grains. There are observational indications that polarization is at a maximum following primary light minimum (Raveendran & Rao 1988; Raveendran, Rao, & Anandaram 1989; Nook, Cardelli, & Nordsieck 1990). Nook et al. argue that, if a fresh episode of grain formation is to account for the polarization change, the grains must form within 0.2 stellar radii of the photosphere. This, they consider, is "uncomfortably close" to the photosphere. In their view, polarization is primarily the result of an asymmetrical photospheric radiation field scattered off the distant dust layer responsible for the infrared excess. Perhaps closer spectroscopic, photometric, and polarimetric scrutiny will show whether and where dust forms during a pulsational cycle, and, perhaps, show dust-gas separation set into action.

Recognizing that dust-gas separation is prevalent among RV A and B stars, it is possible to correct for it in order to arrive at the composition of the star prior to onset of the separation. In particular, one may place the carbon and *s*-process abundances in an evolutionary context. A few RV Tauri variables appear enriched in *s*-process elements but many do not. It, therefore, seems that evolution onto the AGB and experience of the third dredge-up is not a prerequisite for the progenitor of a RV Tauri variable. A star with a low mass envelope may evolve into the instability strip off the horizontal branch or the AGB (Gingold 1976). It may be noteworthy that this requirement of a low mass envelope is one that facilitates the generation of abundance anomalies in the envelope by dust-gas separation. It will be useful to define more fully abundances of those elements most affected during evolution to and on the AGB: C, N, and O as well as a full suite of *s*-process elements with *r*-process elements such as Eu to serve as controls.

This research has been supported in part by the Robert A. Welch Foundation of Houston, Texas, and the National Science Foundation (grant AST 96-18414).

REFERENCES

Alcolea, J., & Bujarrabal, V. 1991, A&A, 245, 499
Baird, S. R. 1981, ApJ, 245, 208
Borisov, Yu. V., & Panchuk, V. E. 1986, Bull. Spec. Ap. Obs., 22, 11
Cardelli, J. A. 1989, AJ, 98, 324
Dawson, D. W. 1979, ApJS, 41, 97
Fokin, A. B. 1994, A&A, 292, 133
Gehrz, R. D. 1972, ApJ, 178, 715
Gehrz, R. D., & Ney, E. P. 1972, PASP, 84, 768
Gingold, R. A. 1976, ApJ, 204, 116
Giridhar, S., & Arellano Ferro, A. 1995, Rev. Mexicana Astron. Astrofis., 31, 23
Giridhar, S., Lambert, D. L., & Gonzalez, G. 1998, PASP, 110, 671
Giridhar, S., Rao, N. K., & Lambert, D. L. 1994, ApJ, 437, 476
Goldsmith, M. J., Evans, A., Albinson, J. S., & Bode, M. F. 1987, MNRAS, 227, 143
Gonzalez, G., & Lambert, D. L. 1997, AJ, 114, 341
Gonzalez, G., Lambert, D. L., & Giridhar, S. 1997a, ApJ, 479, 427
———. 1997b, ApJ, 481, 452
Gonzalez, G., & Wallerstein, G. 1994, AJ, 108, 1325
Grevesse, N., Noels, A., & Sauval, A. J. 1996, ASP Conf. Proc. 99, Cosmic Abundances, ed. S. S. Holt & G. Sonnenborn (San Francisco: ASP), 117
Groenewegen, M. A. T., Smith, C. H., Wood, P. R., Omont, A., Fujiyoshi, T. 1995, ApJ, 449, L119
Gustafsson, B., Bell, R. A., Eriksson, K., & Nordlund, Å. 1975, A&A, 42, 407
Joy, A. H. 1952, ApJ, 115, 25
Jura, M. 1986, ApJ, 309, 732
Kholopov, P. N., Samus, N. N., Durlevich, O. V., Kazarovets, E. V., Kireeva, N. N., & Tsvetkova, T. M. 1985, General Catalogue of Variable Stars (4th ed.; Moscow: Nauka)
Kukarkin, B. V., Parenago, P. P., Yu, N., & Kholopov, P. N. 1958, General Catalogue of Variable Stars (2d ed.; Moscow: Acad. Sci. USSR)
Lambert, D. L. 1989, in AIP Conf. Proc. 183, Cosmic Abundances of Matter, ed. C. J. Waddington (New York: AIP), 168
Lambert, D. L., Heath, J. E., Lemke, M., & Drake, J. 1996, ApJS, 103, 183
Lloyd Evans, T. 1985, MNRAS, 217, 493
Luck, R. E. 1981, PASP, 93, 211
Luck, R. E., & Bond, H. E. 1989, ApJ,342, 476
McCarthy, J. K., Sandiford, B. A., Boyd, D., & Booth, J. 1993, PASP, 105, 881
McWilliam, A. 1997, ARA&A, 35, 503
Nook, M. A., Cardelli, J. A., & Nordsieck. K. H. 1990, AJ, 100, 2004
Percy, J. R. 1993, ASP Conf. Ser. 45 Luminous High-Latitude Stars, ed. D. D. Sasselov (San Francisco: ASP), 295
Percy, J. R., Bezuhly, M., & Milanowski, M. 1997, PASP, 109, 264
Pollard, K. R., Cottrell, P. L., Kilmartin, P. M., & Gilmore, A. C. 1996, MNRAS, 279, 949
Pollard, K. R., Cottrell, P. L., Lawson, W. A., Albrow, M. D., & Tobin, W. 1997, MNRAS, 286, 1
Preston, G. W., Krzeminski, W., Smak, J., & Williams, J. A. 1963, ApJ, 137, 401
Raveendran, A. V. 1989, MNRAS, 238, 943
Raveendran, A. V., & Rao, N. K. 1988, A&A, 192, 259
Raveendran, A. V., Rao, N. K., Anandaram, M. N. 1989, MNRAS, 240, 823
Russell, S. C. 1997, A&A, 326, 1069
Savage, B. D., & Sembach, K. R. 1996, ARA&A, 34, 279
Schmidt, E. G., & Seth, A. 1996, AJ, 112, 2769
Shenton, M., et al. 1992, A&A, 262, 138
Sneden, C. 1973, Ph.D. thesis, Univ. Texas at Austin
Sneden, C., & Crocker, D. A. 1988, ApJ, 335, 406
Spite, M., & Spite, F. 1978, A&A, 67, 23
Tull, R. G., MacQueen, P. J., Sneden, C., & Lambert, D. L. 1995, PASP, 107, 251
Van Winckel, H. 1997, A&A, 319, 561
Van Winckel, H., Waelkens, C., & Waters L. B. F. M. 1995, A&A, 293, L25
Waelkens, C., Van Winckel, H., Trams, N. R., & Waters, L. B. F. M. 1992, A&A, 256, L15
Waelkens, C., & Waters, L. B. F. M. 1993, ASP Conf. Ser. 45 Luminous High-Latitude Stars, ed. D. D. Sasselov (San Francisco: ASP), 219
Wahlgren, G. M. 1992, AJ, 104, 1174
Wasson, J. T. 1985, Meteorites: Their Record of Early Solar System History (New York: Freeman)
Wheeler, J. C., Sneden, C., & Truran, J. W. 1989, ARA&A, 27, 279
Yoshioka, K. 1979, PASJ, 31, 23